Food Chemistry 354 (2021) 129578

Contents lists available at ScienceDirect

Food Chemistry

journal homepage: www.elsevier.com/locate/foodchem

Analytical Methods

A microfluidic colorimetric biosensor for in-field detection of *Salmonella* in fresh-cut vegetables using thiolated polystyrene microspheres, hose-based microvalve and smartphone imaging APP

Yan Man [a,b,c,1,*], Meijing Ban [d,1], An Li [a,b,c], Xinxin Jin [a,b,c], Yuanfang Du [a,b,c], Ligang Pan [a,b,c,*]

[a] Beijing Research Center for Agricultural Standards and Testing, Beijing Academy of Agriculture and Forestry Sciences, Beijing 100097, China
[b] Risk Assessment Lab for Agro-products (Beijing), Ministry of Agriculture. P.R. China, Beijing 100097, China
[c] Beijing Municipal Key Laboratory of Agriculture Environment Monitoring, Beijing 100097, China
[d] School of Food Science and Engineering, Beijing University of Agriculture, Beijing 102206, China

ARTICLE INFO

Keywords:
Microfluidic chip
Polystyrene microsphere
Colorimetric
Foodborne pathogen
Microvalve
Smartphone
Fresh-cut vegetable

ABSTRACT

A microfluidic colorimetric biosensor was developed using thiolated polystyrene microspheres (SH-PSs) for aggregating of gold nanoparticles (AuNPs), a novel hose-based microvalve for controlling the flow direction, and a smartphone imaging APP for monitoring colorimetric signals. Aptamer-PS-cysteamine conjugates were used as detection probes and reacted with *Salmonella* in samples. Complementary DNA - magnetic nanoparticle (cDNA - MNP) conjugates were used as capture probes, reacted with the free aptamer-PS-cysteamine conjugates. AuNPs were aggregated on the surface of *Salmonella*-aptamer-PS-cysteamine conjugates, resulting in a visible color change in the detection chamber, which indicating different concentrations of *Salmonella*. The limit of detection was low to 6.0×10^1 cfu/mL. The microfluidic biosensor exhibited a good specificity. It was evaluated by analyzing salad samples spiked with *Salmonella*. The recoveries ranged from 91.68% to 113.76%, which indicated its potential application in real samples.

1. Introduction

Foodborne diseases mainly caused by 15 foodborne pathogens contamination have become a chronic problem worldwide (Zheng et al., 2019). Foodborne pathogens have become an important food safety concern (Yin et al., 2020). Among all these foodborne pathogens, *Salmonella* is the major cause of foodborne disease outbreaks in human and animal hosts no matter in developing or developed countries (Ansari, Yazdian-Robati, Shahdordizadeh, Wang, & Ghazvini, 2017; Li, Zhang, Tian, & Xu, 2020). However, fresh-cut vegetables are one of the main reservoirs of *Salmonella typhimurium* (Kim & Oh, 2020). With the improvement of living standards, consumers are becoming increasingly concerned about the food safety and nutritive quality of their diet. Hence, consumption of fresh-cut vegetables is rapidly increasing due to their freshness, nutrition, convenience and sensory quality. Hence, it is necessary to self-monitor foodborne pathogens in fresh-cut vegetables to prevent food poisoning.

The commonly used methods for the detection of foodborne pathogens include culture-based method, polymerase chain reaction (PCR) and enzyme-linked immune-sorbent assay (ELISA). They either suffer from 3 to 5 days for obtaining results, or need well-trained technicians and complex DNA extraction procedures, or lack sufficient sensitivity (Hu et al., 2019; Zheng, Cai, Qi, Wang, Wang, & Lin, 2020). Moreover, matrix-assisted laser desorption/ionization time-of-flight mass spectrometry (MALDI-TOF-MS) also was used for the analysis of foodborne pathogens (Kailasa, Koduru, Baek, Wu, Hussain, & Park, 2020). But this method requires large scale equipment and highly qualified technicians. Therefore, it is crucial to develop rapid, simple, sensitive, user-friendly and in-field detection methods of foodborne pathogens to ensure food safety.

Recently, biosensors coupled with a colorimetric, fluorescent, electrochemical or surface plasmon resonance (SPR) transducer, are

* Corresponding authors at: Beijing Research Center for Agricultural Standards and Testing, Beijing Academy of Agriculture and Forestry Sciences, Beijing 100097, China.
E-mail addresses: manyan3669@163.com (Y. Man), panligang2012@126.com (L. Pan).
[1] Yan Man, Meijing Ban contributed equally to this work.

https://doi.org/10.1016/j.foodchem.2021.129578
Received 12 October 2020; Received in revised form 25 February 2021; Accepted 5 March 2021
Available online 14 March 2021

considered to be powerful analytical tools and have attracted a great deal of attention for rapid detecting of foodborne pathogens (Baek et al., 2019, 2020; Liu, Yang, Li, & Du, 2021; Man, Jin, Fu, & Pan, 2019). Microfluidic chip, also called lab-on-a-chip (LOC) or miniaturized total analysis systems (μ-TAS), is very important in biosensors due to its great merits of low consumption of sample and reagent, real-time detection, shortened detection time and miniaturized analytical platform (Kant et al., 2018; Wang et al., 2019; Zhao, Li, & Liu, 2019; Zheng et al., 2019; Zhang, Lv, Yasmeen, Qing, & Deng, 2017). Among them, microfluidic colorimetric biosensors could rapidly produce visible results which can be easily observed with naked eye, spectrometry or smartphone imaging APP for quantitative detection (Man, et al., 2019; Sayad, Ibrahim, Uddin, Cho, Madou, & Thong, 2018; Xia et al., 2019; Zheng et al., 2019).

Gold nanoparticles (AuNPs) are an ideal candidate for the development of colorimetric biosensor based on the sensitivity of the surface plasmon resonance to aggregation state, which causes an obvious color change. Recently, a rapid colorimetric detection method was developed for the detection of bacterial species through the capture of AuNPs by thiolated engineered phages (Peng & Chen, 2019). However, the construction and production process of engineered phages are complicated, time-consuming. For this reason, polystyrene microspheres (PSs) with adjustable particle size, abundant surface functional groups and high chemical stability could be chosen as the alternative for engineered phages. Until now, PSs have been widely used as carriers such as antibodies (Cai et al., 2019), antigens (Sheng, Huang, Liu, Zhang, Zhang, & Wang, 2020), streptavidin (Ahmad et al., 2017), molecular beacons (Wang, Yuan, Xu, Yuan, & Li, 2020), quantum dots (Wang et al., 2018), or as core/shell structures of nanocomposite (Chou, Lin, Hsu, Chang, Lu, & Chen, 2020; Liu et al., 2020). But, thiolated PSs (SH-PSs) have not been used in the colorimetric detection through the capture of AuNPs.

Additionally, many microvalves based on the actuation of electricity (Das & Payne, 2016), magnetism (Nafea, Nawabjan, & Ali, 2018), gas (Kim, Stockton, Jensen, & Mathies, 2016), light (Jadhav et al., 2015), pH (Bayat & Baghani, 2019), phase change materials (Khanjani, Hajarian, Kargar-Estahbanaty, Arbabi, Taheri, & Baghani, 2020) and surface acoustic wave (SAW) (Liu, Fu, Zhang, & Hu, 2017) were developed and applied into microfluidic chips for controlling the flow direction of the fluids. However, there are many disadvantages still existing in those microvalves, such as high energy consumption, high cost, complex structure, many components, easy leakage, large dead zone and non-portability (Qian, Hou, Li, & Jin, 2020). Therefore, it is very necessary to design and establish a simple, low cost, low energy consumption and portable microvalve for microfluidic chips.

Furthermore, aptamers are a class of single-stranded DNA or RNA oligonucleotides that possess high affinity for specific recognition of small molecules, proteins or cells (Cao, Wang, Liu, Xue, & Mao, 2020; Xing, Peng, Shan, Liu, Huang, & Lai, 2020). Compared with monoclonal antibodies, aptamers exhibit several unique features such as easy preparation and modification, good stability, high purity and low cost of production.

Herein, a microfluidic colorimetric biosensor using SH-PSs to aggregate AuNPs to detect *Salmonella typhimurium* has not been reported to the best of our knowledge. Microfluidic chips prepared using Norland Optical Adhesive 81 (NOA 81) and glass substrates, were used for mixing, enrichment and detection of *Salmonella typhimurium*. A novel and simple hose-based microvalve was designed and used for controlling the flow direction of the fluids. Aptamer-PS-cysteamine conjugates were used as detection probes, and allowed the binding of AuNPs which aggregated on the surface of PSs, resulting in a visible color change. Complementary DNA-magnetic nanoparticle (cDNA-MNP) conjugates were used as capture probes and the self-magnetism for rapid separation and purification, which makes the microfluidic chips reusable. This work showed a novel microfluidic colorimetric biosensor which can realize a rapid and in-field detection of *Salmonella typhimurium* within 45 min. The colorimetric signals were captured by smartphone imaging APP and Vis spectroscopy (as a comparison), respectively.

2. Experimental

2.1. Materials and chemicals

NH_2-labelled *Salmonella typhimurium* aptamer (5′-TATGGCGGCGTCACCCGACGGGGACTTGACATTATGACAGAAAAAAAAAA-NH_2-3′) and NH_2-labelled partly complementary DNA (cDNA) of *Salmonella typhimurium* aptamer (5′-TCGGGTGACGCCGCCATAAAAAAAAAAA-NH_2-3′) were purchased from Sangon Biotechnology Co., Ltd. (Shanghai, China). *Salmonella typhimurium* (ATCC 14028), *Staphylococcus aureus* (ATCC25923) and *E. coli O157:H7* (CICC 21530) were ordered from China Center of Industrial Culture Collection (Beijing, China). Carboxyl modified polystyrene microspheres (COOH-PSs) were obtained from Beijing Zhongkeleiming Technology Co., Ltd. (Beijing, China). Carboxyl modified magnetic nanoparticles (COOH-MNPs) were obtained from Thermo Fisher Scientific (Shanghai, China). Tween-20 was bought from Alfa Aesar Chemical Co., Ltd. (Shanghai, China). Norland Optical Adhesive 81 (NOA 81) was bought from Norland Products Inc. (NJ, USA). Tris (2-carboxyethyl) phosphine (TCEP), cysteamine, 1-ethyl-3-(3-dimethylaminopropyl)-carbodiimide hydrochloride (EDC), *N*-hydroxysuccinimide (NHS) and gold chloride ($HAuCl_4{\cdot}3H_2O$) were ordered from Sigma-Aldrich Chemical Co. (St. Louis, MO). Sodium citrate was bought from AMRESCO (OH, USA). Water was purified with a Milli-Q apparatus (Molsheim, France). Moreover, the glass substrates (80 mm × 45 mm) were purchased from Luoyang Guluo Glass Co., Ltd (Henan, China). Chrome blanks (120 mm × 120 mm) were bought from Changsha Shaoguang Chrome Blank Co., Ltd (Hunan, China).

2.2. Preparation of microfluidic chips

The microfluidic chips were prepared following a previously reported method using Mask Aligner (JKG-2A, Shanghai, China, http://www.xueze.com/) (Man et al., 2019). The fabrication process was shown in Fig. S1. The cofferdams and photomask **a**, **b** and **c** (Fig. S1C) were designed using Adobe Illustrator CC. The cofferdams were used to control the thickness of microfluidic chips. To fabricate the first layer (Fig. S1A), a cofferdam was fixed on the chromium plate by UV curing. 0.3 mL of NOA81 was put into the cofferdam, photomask **a** was pressed onto the NOA81. Significantly, there should be no bubbles between NOA81 and photomask. After UV exposure 21 s, the NOA81 layer, photomask **a** and cofferdam were gently torn together from chromium plate. The cofferdam was stripped off, uncured NOA81 was rinsed thoroughly by the mixture of acetone and ethyl alcohol (v: v = 5:1). After dried, the first layer which left on photomask **a** was prepared. The second layer was prepared using photomask **b**, and the preparation process is the same as that for the first layer. To fabricate the third layer, two cofferdams were superimposed and fixed on the glass substrate. 0.5 mL of NOA81 was put into the cofferdams, and then photomask **c** was pressed onto the NOA81. After UV exposure 30 s, photomask **c** and cofferdams were stripped off, and then uncured NOA81 was rinsed thoroughly. The third layer was fabricated on the glass substrate. To assemble a microfluidic chip (Fig. S1B). Firstly, the second layer was assembled with the third layer by UV curing 30 s. Photomask **b** was stripped off. Secondly, the first layer was assembled with the second layer by UV curing 60 s. After photomask **a** was stripped off from the top layer, the preparation of microfluidic chip was completed.

2.3. Preparation of AuNPs, cDNA-MNP and cysteamine-PS-aptamer conjugates

Four different particle sizes of AuNPs were prepared as follows. Briefly, 1.0, 0.75, 0.5 and 0.38 mL of 1% (m/v) trisodium citrate were quickly added to 50 mL 0.01% (m/v) of boiling $HAuCl_4$ solution under continuous stirring. When the color changed from pale yellow over black to red, the mixture solution was kept boiling for another 8 min. Finally, four different particle sizes of AuNPs solution were stored at 4 ℃ for

further use.

cDNA-MNP conjugates were prepared according to the following procedures. EDC/NHS mixture solution was prepared by adding 7.67 mg of EDC and 21.7 mg of NHS into 25 mL H_2O. Then 600 μL of EDC/NHS mixture solution and 600 μL of phosphate buffer (PB, pH 5.5, 10 mM) were added into 300 μL of COOH-MNPs (10 mg/mL), the mixture was incubated for 1 h. Following this, 50 μL of cDNA (0.1 μM) was added into the mixture solution, and then the mixture was stirred for another 2 h. Finally, the MNPs mixture was blocked by 100 μL of BSA solution (0.1 mg/mL) for 30 min. The cDNA-MNP conjugates were separated and rinsed thoroughly with PB (pH 7.5, 10 mM) containing 0.01% Tween-20. The prepared cDNA-MNP conjugates were resuspended in 3.3 mL PB buffer (pH 7.5, 10 mM) and were stored at 4 ℃ for further study.

Cysteamine-PS-aptamer conjugates were prepared as follows: 1.5 mL of EDC/NHS mixture solution and 1.5 mL of PB (pH 5.5, 10 mM) were added into 100 μL of COOH-PSs (50 mg/mL), the mixture was incubated for 1 h. To activate the sulfhydryl group, 10 μL of 1 mM TCEP was incubated with 50 μL of aptamer (0.1 μM) and 50 μL of cysteamine (0.1 μM) for 30 min, respectively. Following this, the activated aptamer and cysteamine were added into the PSs mixture solution, and then the mixture was stirred for another 2 h. Finally, the cysteamine-PS-aptamer conjugates were also blocked by 100 μL of BSA solution (0.1 mg/mL) for 30 min. The cysteamine-PS-aptamer conjugates were rinsed thoroughly with PB (PH 7.5, 10 mM) containing 0.01% Tween-20 for four times by centrifugation at 9000 rpm for 20 min. The cysteamine-PS-aptamer conjugates were resuspended in 10 mL PB (pH 7.5, 10 mM) and were stored at 4 ℃ for further use.

2.4. Optimization of experimental conditions

The influence factors, including the sizes of AuNPs and PSs, the concentration of Aptamer-PS-cysteamine conjugates, the incubation time of AuNPs were determined prior to microfluidic colorimetric detection in order to achieve the optimal sensitivity. Respective procedures were given in the Electronic Supporting Material.

2.5. Salmonella typhimurium detection with microfluidic colorimetric biosensor

The standard sample solutions of *Salmonella typhimurium* with different concentrations were prepared by diluting *Salmonella typhimurium* with 10 mM sterile PB (pH 7.5) to the final concentrations from 6.0×10^1 to 6.0×10^7 cfu/mL. 30 μL of *Salmonella typhimurium* standard sample and 30 μL of aptamer-PS-cysteamine conjugates (0.25 mg/mL) were flowed into the microfluidic chip at the same time under the drive of syringe pump (TS-1A, Longer, China, http://www.pumpsystem.cn/). *Salmonella typhimurium* and aptamer-PS-cysteamine conjugates were incubated firstly in the first micro-mixing channel. Then the formed *Salmonella typhimurium*-aptamer-PS-cysteamine conjugates and the rest of aptamer-PS-cysteamine conjugates flowed into the reaction chamber with 20 μL of cDNA-MNP conjugates, the cDNA-MNP conjugates will capture the rest of aptamer-PS-cysteamine conjugates. After magnetic separation, 60 μL of supernatant with *Salmonella* typhimurium-aptamer-PS-cysteamine conjugates was incubated with 60 μL of twice-condensed AuNPs in the second micro-mixing channel. The color change of aggregated AuNPs was determined by a smartphone imaging APP and a multimode plate reader, respectively. All experiments were conducted in triplicate. All injection solutions, mainly including reaction solutions, cleaning solutions and sample solutions, were flowed into the channel of microfluidic chip with the flow speed of 15 μL/min under the drive of syringe pump. The slow flow rate of the injection solutions will ensure adequate mixing, incubation and reaction between solutions, and create a small pressure on the proposed hose-based valve and the entire microfluidic system.

2.6. Preparation of spiked fresh-cut vegetable salad samples

Fresh-cut vegetable salad samples sealed in plastic boxes were purchased from local retail supermarkets in Beijing. 25 g of salad was added into 225 mL of PB in conical flask. After stirring and incubating for 2 min, the supernatant was collected. *Salmonella typhimurium* was then spiked into the supernatant at a final concentration of 0, 6.0×10^1, 6.0×10^2 and 6.0×10^3 cfu/mL, respectively. The spiked salad samples were detected using the proposed microfluidic colorimetric biosensor according to the protocol in Section 2.5.

3. Results and discussion

3.1. Detection strategy of the designed microfluidic colorimetric sensor

The structural diagram of the designed microfluidic chip is shown in Fig. 1A. The microfluidic chip with a dimension of 76 mm × 37 mm mainly consists of a reaction chamber, a colorimetric detection chamber, a hose-based microvalve and two micro-mixing channels. cDNA-MNP conjugates were loaded into the reaction chamber. Moreover, the transparent silicone tubes (1 mm o.d. × 0.5 mm i.d.) were inserted into the inlets (**a**, **b** and **d**), outlet (**c**) and hose-based microvalve. The tubes of inlets are connected to the syringe pump. The sample (inlet **a**), aptamer-PS-cysteamine conjugates (inlet **b**) and AuNPs (inlet **d**) were flowed into the microfluidic chip under the drive of syringe pump. The outlet **c** serves as an outlet for waste liquid and air.

The detection strategy of microfluidic colorimetric sensor for *Salmonella typhimurium* detection is illustrated in Fig. 1B. When *Salmonella typhimurium* is present in sample, they will combine with aptamer-PS-cysteamine conjugates in the first micro-mixing channel. After magnetic separation, large numbers of *Salmonella typhimurium*-aptamer-PS-cysteamine conjugates are present in supernatant. When the supernatant was incubated with AuNPs in the second micro-mixing channel, the sulfhydryl groups of cysteamine will capture AuNPs. The aggregation of AuNPs on the surface of PSs leads to a colorimetric signal (color change) in the colorimetric detection chamber. Conversely, when *Salmonella typhimurium* is not present in sample, the aptamer-PS-cysteamine conjugates will be combined with cDNA-MNP conjugates. After magnetic separation, there are no aptamer-PS-cysteamine conjugates in supernatant. Thus, AuNPs keep the red color in the colorimetric detection chamber. The color changes of the aggregated AuNPs are proportional to the concentration of *Salmonella typhimurium*. The color changes of aggregated AuNPs were captured by smartphone imaging APP and Vis spectroscopy, respectively.

3.2. Design and fabrication of the hose-based microvalve

Microvalves are often used for controlling the flow direction of the fluids. The schematic diagram of the designed and fabricated hose-based microvalve is shown in Fig. 2. The hose-based microvalve consists of two transparent silicone tubes (1 mm o.d. × 0.5 mm i.d.), a rubber hose (2 mm o.d. × 0.8 mm i.d.) and two holes (**a** and **b**) which connected with the channels. The structure of hole **a** and **b** is the same with inlets. Two transparent silicone tubes (1.3 cm long) were inserted into the hole **a** and **b**, respectively. Subsequently, both ends of the rubber hose (3.5 cm long) were connected to the above two transparent silicone tubes. When the microvalve is opened, the solution in the channel can flow through microvalve. Whereas, the solution can not flow through microvalve when it is closed by a 1.5 cm of binder clip. In order to evaluate the stability of the developed microvalve, the microfluidic system was continuously injected for 72 h at the flow rate of 15 μL/min. The results showed that the microvalve and pipelines remained stable without leakage. Moreover, we carried out experiments at the flow rate of 100, 500, 1000 and 2000 μL/min for three times, respectively. The proposed hose-based microvalves still remained in a stable state without leakage. This may be attributed to the positive anchoring of NOA81 for the

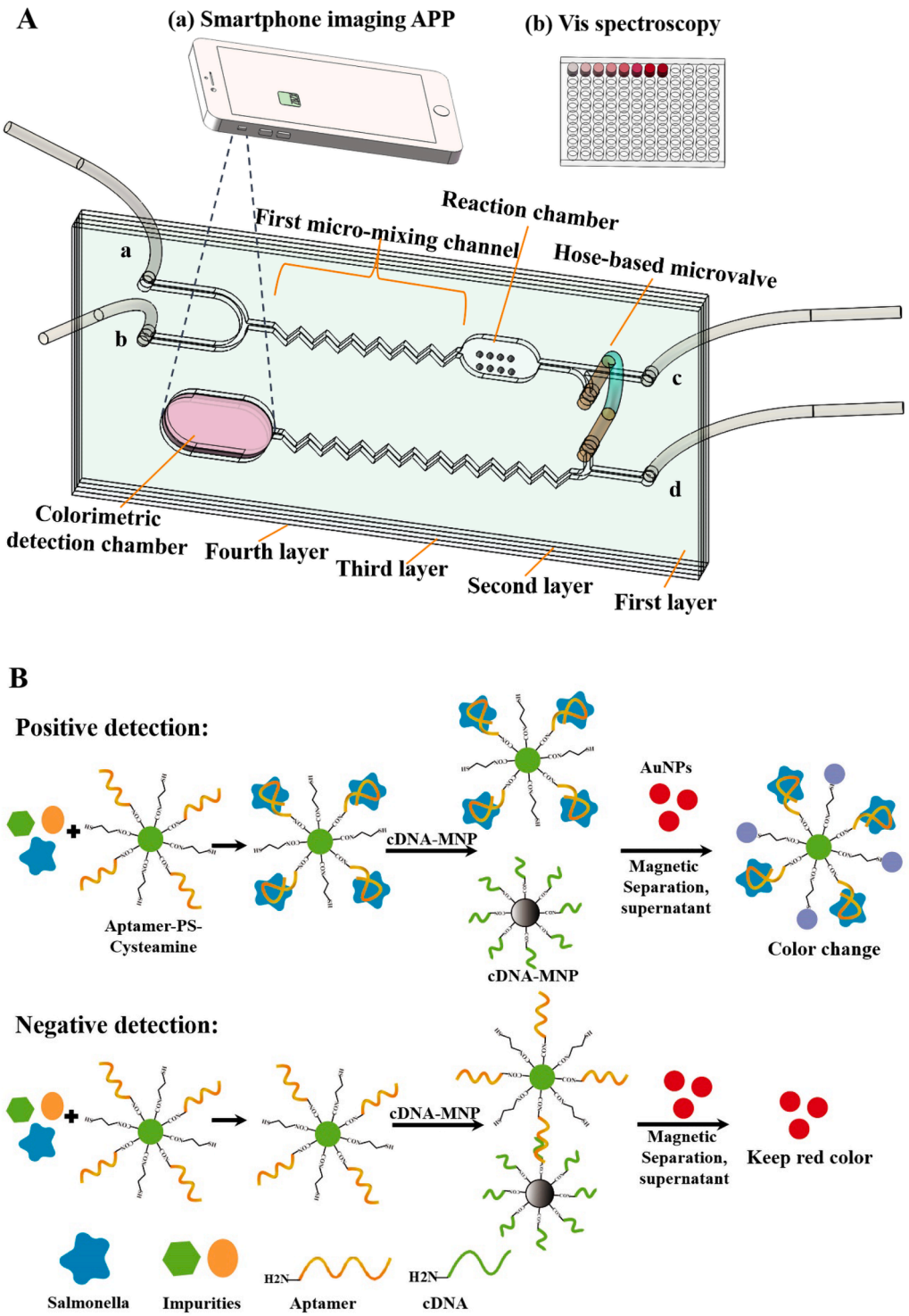

Fig. 1. The schematic of the proposed microfluidic colorimetric biosensor for the detection of *Salmonella typhimurium* based on SH-PSs, hose-based microvalve and smartphone imaging APP. (A) The 3 D structural of the designed microfluidic chip; (B) The detection strategy of the microfluidic colorimetric biosensor by using SH-PSs to aggregate AuNPs for the detection of *Salmonella typhimurium*.

microvalves and pipelines. Hence, the proposed hose-based valve and the entire microfluidic system are in a stable state. Compared with the reported electricity (Das & Payne, 2016), magnetism (Nafea et al., 2018), gas (J. Kim et al., 2016), light (Jadhav et al., 2015), pH (Bayat & Baghani, 2019) driven microvalves, this hose-based microvalve has shown the merits of simple structure, low cost fabrication, simple operation, low energy consumption, low leakage rate and so on.

3.3. Characteristic of nanomaterials and optimization of method

AuNPs of four different sizes (68 nm, 43 nm, 25 nm and 15 nm) (Table S1, Fig. S2), PSs of three different sizes (100 nm, 400 nm and 1000 nm) (Fig. S3) and MNPs (1000 nm) (Fig. S4 and Fig. S5) were characterized by transmission electron microscopy (TEM, FEI Tecnai G2 F30, USA, https://www.fei.com/), Vis spectrum (Envision, PerkinElmer, https://www.perkinelmer.com.cn/) or laser particle size analyzer

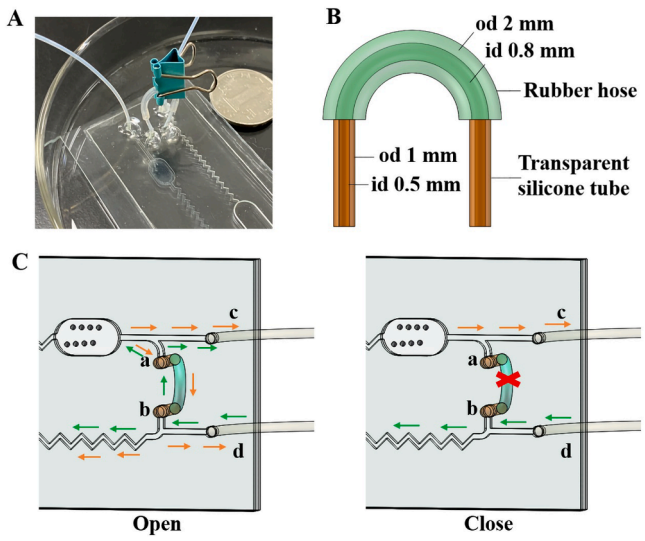

Fig. 2. Schematic diagram of the hose-based microvalve. (A) The image of fabricated microvalve for microfluidic chip; (B) The 3 D structural diagram of the designed microvalve; (C) The flow directions of the fluid when the microvalve was open and closed.

(LPSA, Zetasizer Nano ZS90, USA, http://www.thermofisher.com), respectively. Respective data were given in the Electronic Supporting Material.

After optimization, the following experimental conditions were found to give best results: (a) AuNPs size of 25 nm (Fig. S6A); (b) PSs size of 100 nm (Fig. S6B); (c) Aptamer-PS-cysteamine concentration of 18.2 ng/mL (Fig. S6C); (d) Incubation time for 20 min (Fig. S6D).

3.4. *Salmonella typhimurium* detection with microfluidic colorimetric biosensor by smartphone imaging APP

Salmonella typhimurium stored in ceramic bead strains storage tube at −20°C, was revived and grown in 5 mL of Brian Heart Infusion (BHI) broth at 37 °C for activation. After 24 h, the *Salmonella typhimurium* was serially 10-fold diluted with the sterile PB (10 mM, pH 7.5) to the final concentrations from 0 to 6.0×10^7 cfu/mL. Moreover, a portable smartphone imaging APP based on Hue-Saturation-Lightness (HSL) mode was developed for image processing. Furthermore, the saturations of red color space in colorimetric detection chamber were used for image analysis in this paper. This APP was loaded on the Android smartphone (Vivo Z5, Resolution: 2340 × 1080 pixels, Guangdong, China). The smartphone was fixed above the microfluidic chip. The angle between microfluidic chip and smartphone was 20°. The vertical distance between the microfluidic chip and smartphone camera was 6.5 cm. Moreover, in order to get better color rendering effect, we used an adjustable led light to control the intensity of the light, and put a piece of white paper under the microfluidic chip.

The prepared microfluidic chip was shown in Fig. 3A. Under the optimal conditions, different concentrations of *Salmonella typhimurium* ranging from 0 to 6.0×10^7 cfu/mL were detected using this proposed microfluidic colorimetric biosensor by smartphone imaging APP according to the procedures described in the Experimental section. As shown in Fig. 3B, the red color of the AuNPs changed from deep to shallow when the concentrations of *Salmonella typhimurium* increased from 0 to 6.0×10^7 cfu/mL. Furthermore, the color changes of the AuNPs were measured by the smartphone imaging APP to obtain their saturations. As shown in Fig. 3 C and D, the saturation was found to have a good linear relationship with the concentration of *Salmonella typhimurium* ranging from 6.0×10^1 to 6.0×10^5 cfu/mL. The calibration curve could be described as $S = -2.01 \lg C_{\textit{Salmonella typhimurium}} + 17.8$ with a correlation coefficient of 0.9966. The low detection limit of this proposed microfluidic colorimetric biosensor by smartphone imaging APP was about 6.0×10^1 cfu/mL.

Additionally, Table S2 summarized the comparison of the different microfluidic biosensors for the detection of foodborne pathogens. Similar results were found for some foodborne pathogens detection using microfluidic biosensor by smartphone imaging APP. For example, the detection limits of 50 cfu/mL and 58 cfu/mL were obtained for *Escherichia coli O157:H7* (Zheng, Cai, Wang, Liao, Li, & Lin, 2019) and

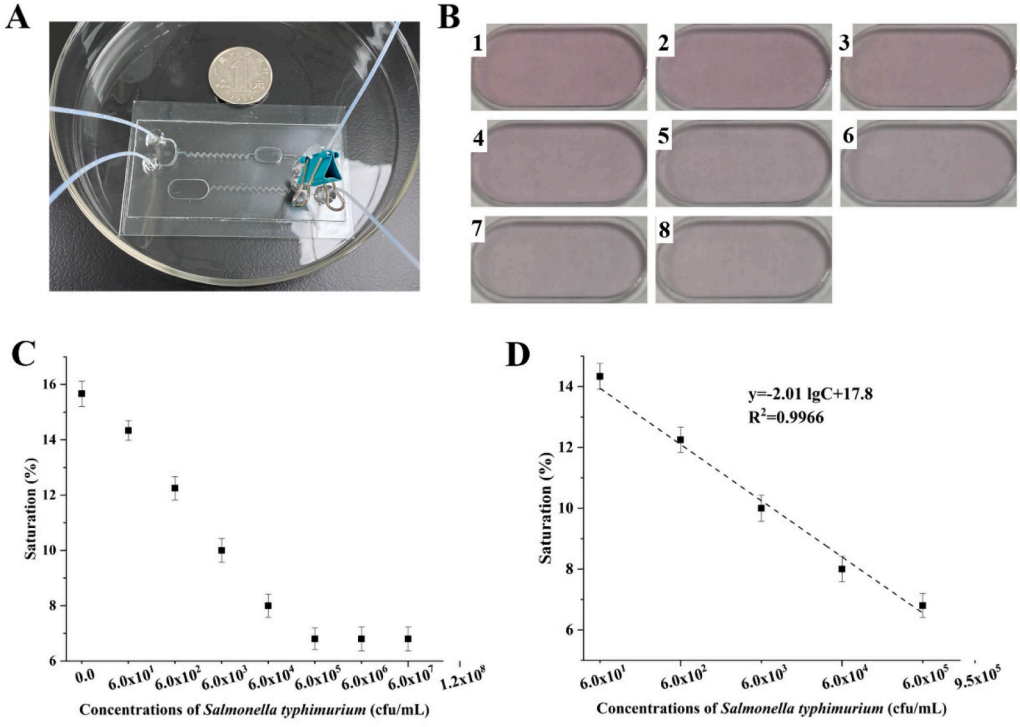

Fig. 3. *Salmonella typhimurium* detection with microfluidic colorimetric biosensor by smart phone imaging APP. (A) The image of prepared microfluidic chip; (B) The image of the AuNPs solution in the colorimetric detection chamber which captured by smart phone imaging APP. The concentrations of *Salmonella typhimurium* from **1** to **8** were 0, 6.0×10^1, 6.0×10^2, 6.0×10^3, 6.0×10^4, 6.0×10^5, 6.0×10^6 and 6.0×10^7 cfu/mL, respectively; (C) The saturation of the AuNPs solution in the colorimetric detection chamber versus the different concentrations of *Salmonella typhimurium* (0, 6.0×10^1, 6.0×10^2, 6.0×10^3, 6.0×10^4, 6.0×10^5, 6.0×10^6 and 6.0×10^7 cfu/mL); (D) Linear correlation between the saturation of the AuNPs solution and *Salmonella typhimurium* concentrations. Vertical bars indicate the standard deviation ($n = 3$).

Salmonella typhimurium (Wang et al., 2019), respectively. Furthermore, the developed microfluidic biosensor in this work had a shorter detection time.

3.5. *Salmonella typhimurium* detection with microfluidic colorimetric biosensor by vis spectroscopy

In order to evaluate the sensitivity of the microfluidic colorimetric biosensor by smartphone imaging APP, different concentrations of *Salmonella typhimurium* ranging from 0 to 6.0×10^7 cfu/mL were also quantitatively analyzed using the microfluidic colorimetric biosensor by Vis spectroscopy. 100 μL of the aggregated AuNPs solutions in the colorimetric detection chambers were collected into a 96 well microplate and detected at the wavelength of 400–700 nm by a multimode plate reader. The results were shown in Fig. 4. With the increase of *Salmonella typhimurium* concentrations from 0 to 6.0×10^5 cfu/mL, the absorbances of AuNPs solutions decreased rapidly. Moreover, the absorbances basically kept unchanged when the concentrations of *Salmonella typhimurium* increased from 6.0×10^5 to 6.0×10^7 cfu/mL. The absorbance is found to have a good linear relationship with the concentration of *Salmonella typhimurium* ranging from 6.0×10^1 to 6.0×10^5 cfu/mL, the linear equation was fitted to Ab = -0.0189 lgC $_{Salmonella\ typhimurium}$ + 0.3242 with a correlation coefficient of 0.9976. The limit of detection (LOD) for *Salmonella typhimurium* is about at 6.0×10^1 cfu/mL. Hence, the sensitivity of the proposed microfluidic colorimetric biosensor by smartphone imaging APP was similar to that of Vis spectroscopy. The LODs for both of them were 6.0×10^1 cfu/mL, but the detection of Vis spectroscopy had a wider linear range.

3.6. Specificity of the microfluidic colorimetric biosensor

The specificity of this microfluidic colorimetric biosensor was evaluated using two common foodborne pathogens (*E. coli O157:H7* and *Staphylococcus aureus*) and their mixtures with *Salmonella typhimurium*. The similar concentration (6.0×10^4 cfu/mL) of the *Salmonella typhimurium*, *E. coli O157:H7*, *Staphylococcus aureus* and their mixtures were analyzed by the microfluidic colorimetric biosensor by smartphone imaging APP and Vis spectroscopy, respectively. As shown in Fig. 5, the significant changes of saturation and absorbance were only observed in these samples with *Salmonella typhimurium*. The changes of saturation and absorbance of these samples with only nontarget bacteria were close to that of the control. The results indicated that this proposed microfluidic colorimetric biosensor had a good specificity.

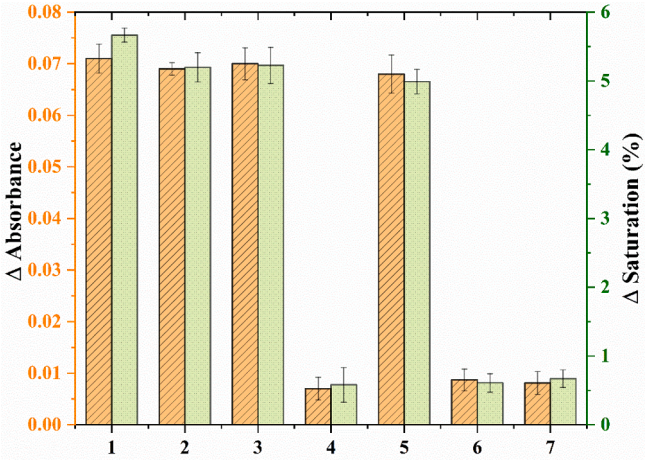

Fig. 5. Specificity of the microfluidic colorimetric biosensor for *Salmonella typhimurium* and two common foodborne pathogens (*E. coli O157:H7* and *Staphylococcus aureus*) by smartphone imaging APP and Vis spectroscopy. 1: Control; 2: *E. coli O157:H7*; 3: *Staphylococcus aureus*; 4: *Salmonella typhimurium*;5: *E. coli O157:H7* and *Staphylococcus aureus*; 6: *E. coli O157:H7* and *Salmonella typhimurium*; 7: *Staphylococcus aureus* and *Salmonella typhimurium*. Vertical bars indicate the standard deviation ($n = 3$).

3.7. Detection of Salmonella typhimurium in the spiked salad samples

To further verify the applicability, the microfluidic colorimetric biosensor was used for the detection of spiked fresh-cut vegetable salad samples by smartphone imaging APP and Vis spectroscopy. The reconstituted *Salmonella typhimurium* in salad samples at the concentration of 0, 6.0×10^1, 6.0×10^2 and 6.0×10^3 cfu/mL were analyzed. The recoveries of the *Salmonella typhimurium* were calculated as the ratio of the detected concentrations to the spiked concentrations. The detection results of the microfluidic colorimetric biosensor by smartphone imaging APP and Vis spectroscopy were shown in Table 1. The recoveries of the proposed microfluidic colorimetric biosensor range from 91.68% to 113.76% for smartphone imaging APP, and from 90.63% to 105.46% for Vis spectroscopy. Hence, the developed microfluidic colorimetric biosensor can be reliable and useful for the detection of *Salmonella typhimurium* in fresh-cut vegetable samples.

4. Conclusions

In summary, we have successfully developed a microfluidic

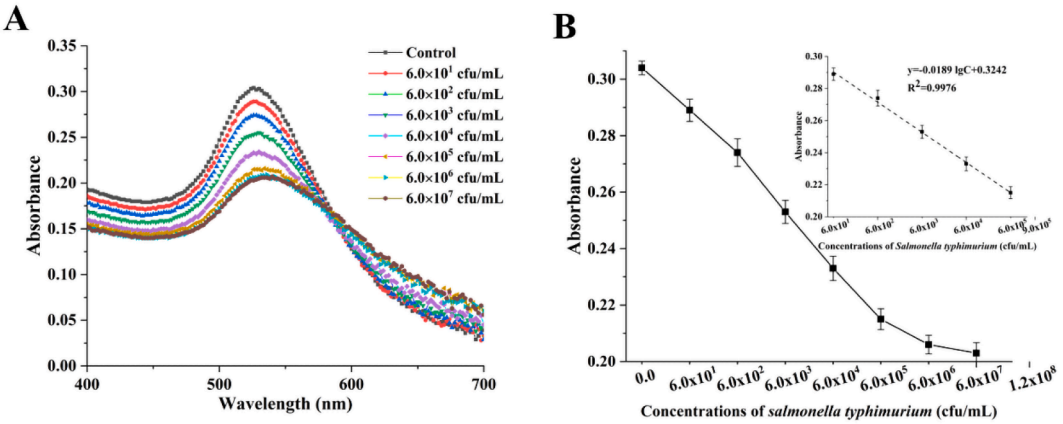

Fig. 4. *Salmonella typhimurium* detection with microfluidic colorimetric biosensor by UV–Vis spectroscopy. (A) Vis absorption spectrum of the AuNPs solution with different concentrations of *Salmonella typhimurium* (0, 6.0×10^1, 6.0×10^2, 6.0×10^3, 6.0×10^4, 6.0×10^5, 6.0×10^6 and 6.0×10^7 cfu/mL); (B) Absorbance of the AuNPs solution versus the concentrations of *Salmonella typhimurium*. Moreover, the linear correlation between absorbance of AuNPs solution in the colorimetric detection chamber and *Salmonella typhimurium* concentrations. Vertical bars indicate the standard deviation ($n = 3$).

Table 1
The microfluidic colorimetric biosensor for the detection of *Salmonella typhimurium* in salad samples by smart phone imaging APP and Vis spectroscopy ($n = 3$).

Sample	Spiked(cfu/mL)	Smart phone imaging APP			Vis spectroscopy		
		Detected(cfu/mL)	Recovery(%)	RSD(%)	Detected(cfu/mL)	Recovery(%)	RSD(%)
1	0	ND[a]	–	–	ND	–	–
2	0	ND	–	–	ND	–	–
3	6.0×10^1	56	93.38	3.39	58	96.01	3.06
4	6.0×10^1	55	91.68	4.23	58	96.42	2.12
5	6.0×10^2	557	92.85	4.26	556	92.60	5.84
6	6.0×10^2	682	113.76	6.75	633	105.46	3.09
7	6.0×10^3	6457	107.61	4.57	5444	90.63	3.53
8	6.0×10^3	6761	112.68	5.90	5733	95.55	3.53

[a] ND: Not detectable.

colorimetric biosensor for rapid and in-field detection of foodborne pathogens in fresh-cut vegetables based on thiolated PSs, hose-based microvalve and smartphone imaging APP. Under the optimal conditions, the proposed microfluidic colorimetric biosensor was able to detect *Salmonella typhimurium* as low as 6.0×10^1 cfu/mL within about 45 min. The recoveries ranged from 91.68% to 113.76% for the spiked fresh-cut vegetables salad samples. The designed microfluidic biosensor had shown the merits of simple structure and operation of microvalve for controlling the flow direction of the fluids, portable and small of smartphone imaging APP for data processing and output, small size and low cost of microfluidic chip device for the integration for sample and reagent handling and in-field detection. At present, the proposed microfluidic colorimetric biosensor was not able to meet the demand on the detection limit of 1 cfu/mL for practical applications, but it could be combined with immunomagnetic separation and concentration of the target bacteria to further improve the sensitivity in the future work. Additionally, this microfluidic device could be further improved by miniaturizing and integrating of the same fluid flow paths and using their specific aptamers for the high-throughput detection of foodborne pathogens.

CRediT authorship contribution statement

Yan Man: Data curation, Methodology, Writing - original draft, Funding acquisition. **Meijing Ban:** Data curation, Formal analysis. **An Li:** Investigation, Resources, Project administration. **Xinxin Jin:** Methodology, Investigation, Project administration. **Yuanfang Du:** Conceptualization, Methodology, Resources. **Ligang Pan:** Methodology, Funding acquisition, Supervision.

Declaration of Competing Interest

The authors declare that they have no known competing financial interests or personal relationships that could have appeared to influence the work reported in this paper.

Acknowledgments

This study was funded by National Natural Science Foundation of China (31801618), Special Projects of Construction of Science and Technology Innovation Ability of Beijing Academy of Agriculture and Forestry Sciences (KJCX20200409), Beijing Municipal Excellent Talents Foundation (2016000020060G127).

Appendix A. Supplementary data

Supplementary data to this article can be found online at https://doi.org/10.1016/j.foodchem.2021.129578.

References

Ahmad, R., Destgeer, G., Afzal, M., Park, J., Ahmed, H., Jung, J. H., Park, K., Yoon, T.-S., & Sung, H. J. (2017). Acoustic wave-driven functionalized particles for aptamer-based target biomolecule separation. *Analytical Chemistry, 89*(24), 13313–13319. https://doi.org/10.1021/acs.analchem.7b0347410.1021/acs.analchem.7b03474.s001.

Ansari, N., Yazdian-Robati, R., Shahdordizadeh, M., Wang, Z., & Ghazvini, K. (2017). Aptasensors for quantitative detection of *Salmonella typhimurium*. *Analytical Biochemistry, 533*, 18–25. https://doi.org/10.1016/j.ab.2017.06.008.

Baek, S. H., Kim, M. W., Park, C. Y., Choi, C. S., Kailasa, S. K., Park, J. P., & Park, T. J. (2019). Development of a rapid and sensitive electrochemical biosensor for detection of human norovirus via novel specific binding peptides. *Biosensors and Bioelectronics, 123*, 223–229. https://doi.org/10.1016/j.bios.2018.08.064.

Baek, S. H., Park, C. Y., Nguyen, T. P., Kim, M. W., Park, J. P., Choi, C., … Park, T. J. (2020). Novel peptides functionalized gold nanoparticles decorated tungsten disulfide nanoflowers as the electrochemical sensing platforms for the norovirus in an oyster. *Food Control, 114*, 107225. https://doi.org/10.1016/j.foodcont.2020.107225.

Bayat, M. R., & Baghani, M. (2019). Fully-coupled transient fluid-solid interaction simulation of the pH-sensitive hydrogel-based microvalve. *International Journal of Applied Mechanics, 11*(07), 1950071. https://doi.org/10.1142/S1758825119500716.

Cai, G., Zheng, L., Liao, M., Li, Y., Wang, M., Liu, N., & Lin, J. (2019). A microfluidic immunosensor for visual detection of foodborne bacteria using immunomagnetic separation, enzymatic catalysis and distance indication. *Microchimica Acta, 186*(12), 757. https://doi.org/10.1007/s00604-019-3883-x.

Cao, Z., Wang, S., Liu, Z., Xue, C., & Mao, X. (2020). A rapid, easy, and sensitive method for detecting His-tag-containing chitinase based on ssDNA aptamers and gold nanoparticles. *Food Chemistry, 330*, Article 127230. https://doi.org/10.1016/j.foodchem.2020.127230.

Chou, P.-C., Lin, F.-P., Hsu, H.-L., Chang, C.-J., Lu, C.-H., & Chen, J.-K. (2020). Electrorheological sensor encapsulating microsphere media for plague diagnosis with rapid visualization. *ACS Sensors, 5*(3), 665–673. https://doi.org/10.1021/acssensors.9b0152910.1021/acssensors.9b01529.s001.

Das, C., & Payne, F. (2016). Design and characterization of low power, low dead volume electrochemically-driven microvalve. *Sensors and Actuators A: Physical, 241*, 104–112. https://doi.org/10.1016/j.sna.2016.01.038.

Hu, J., Jiang, Y.-Z., Tang, M., Wu, L.-L., Xie, H.-Y., Zhang, Z.-L., & Pang, D.-W. (2019). Colorimetric-fluorescent-magnetic nanosphere-based multimodal assay platform for *Salmonella* detection. *Analytical Chemistry, 91*(1), 1178–1184. https://doi.org/10.1021/acs.analchem.8b0515410.1021/acs.analchem.8b05154.s001.

Jadhav, A. D., Yan, B., Luo, R.-C., Wei, L.i., Zhen, X.u., Chen, C.-H., & Shi, P. (2015). Photoresponsive microvalve for remote actuation and flow control in microfluidic devices. *Biomicrofluidics, 9*(3), 034114. https://doi.org/10.1063/1.4923257.

Kailasa, S. K., Koduru, J. R., Baek, S. H., Wu, H. F., Hussain, C. M., & Park, T. J. (2020). Review on matrix-assisted laser desorption/ionization time-of-flight mass spectrometry for the rapid screening of microbial species: A promising bioanalytical tool. *Microchemical Journal, 159*, Article 105387. https://doi.org/10.1016/j.microc.2020.105387.

Kant, K., Shahbazi, M.-A., Dave, V. P., Ngo, T. A., Chidambara, V. A., Than, L. Q., … Wolff, A. (2018). Microfluidic devices for sample preparation and rapid detection of foodborne pathogens. *Biotechnology Advances, 36*(4), 1003–1024. https://doi.org/10.1016/j.biotechadv.2018.03.002.

Khanjani, E., Hajarian, A., Kargar-Estahbanaty, A., Arbabi, N., Taheri, A., & Baghani, M. (2020). Design and fluid-structure interaction analysis for a microfluidic T-junction with chemo-responsive hydrogel valves. *Applied Mathematics and Mechanics, 41*(6), 939–952. https://doi.org/10.1007/s10483-020-2618-6.

Kim, J.-H., & Oh, S.-W. (2020). Rapid and sensitive detection of *E. coli O157:H7* and *S. typhimurium* in iceberg lettuce and cabbage using filtration, DNA concentration, and qPCR without enrichment. *Food Chemistry, 327*, 127036. https://doi.org/10.1016/j.foodchem.2020.127036.

Kim, J., Stockton, A. M., Jensen, E. C., & Mathies, R. A. (2016). Pneumatically actuated microvalve circuits for programmable automation of chemical and biochemical analysis. *Lab on a Chip, 16*(5), 812–819. https://doi.org/10.1039/C5LC01397F.

Li, S., Zhang, Y., Tian, J., & Xu, W. (2020). Luminescent DNAzyme and universal blocking linker Super Polymerase Chain Reaction visual biosensor for the detection

of *Salmonella*. *Food Chemistry, 324*, Article 126859. https://doi.org/10.1016/j.foodchem.2020.126859.

Liu, M., Yang, Z., Li, B., & Du, J. (2021). Aptamer biorecognition-triggered hairpin switch and nicking enzyme assisted signal amplification for ultrasensitive colorimetric bioassay of kanamycin in milk. *Food Chemistry, 339*, Article 128059. https://doi.org/10.1016/j.foodchem.2020.128059.

Liu, W. Y., Fu, X. T., Zhang, X. Q., & Hu, W. Y. (2017). A new microvalve controlled by surface acoustic wave. *Ferroelectrics, 515*(1), 151–158. https://doi.org/10.1080/00150193.2017.1367241.

Liu, X., Yang, J., Li, Q., Wang, Y., Wang, Y., Li, G.e., … Zhang, G. (2020). A strip test for the optical determination of influenza virus H_3 subtype using gold nanoparticle coated polystyrene latex microspheres. *Microchimica Acta, 187*(5). https://doi.org/10.1007/s00604-020-04255-1.

Man, Y., Jin, X., Fu, H., & Pan, L. (2019). A magnetic nanoparticle based immunoassay for alternariol monomethyl ether using hydrogen peroxide-mediated fluorescence quenching of CdTe quantum dots. *Microchimica Acta, 186*(4), 221. https://doi.org/10.1007/s00604-019-3334-8.

Man, Y., Li, A., Li, B., Liu, J., & Pan, L. (2019). A microfluidic colorimetric immunoassay for sensitive detection of altenariol monomethyl ether by UV spectroscopy and smart phone imaging. *Analytica Chimica Acta, 1092*, 75–84. https://doi.org/10.1016/j.aca.2019.09.039.

Nafea, M., Nawabjan, A., & Ali, M. S. M. (2018). A wirelessly-controlled piezoelectric microvalve for regulated drug delivery. *Sensors and Actuators A: Physical, 279*, 191–203. https://doi.org/10.1016/j.sna.2018.06.020.

Peng, H., & Chen, I. A. (2019). Rapid colorimetric detection of bacterial species through the capture of gold nanoparticles by chimeric phages. *ACS Nano, 13*(2), 1244–1252. https://doi.org/10.1021/acsnano.8b06395.

Qian, J. Y., Hou, C. W., Li, X. J., & Jin, Z. J. (2020). Actuation mechanism of microvalves: A review. *Micromachines, 11*(2), 172. https://doi.org/10.3390/mi11020172.

Sayad, A., Ibrahim, F., Uddin, S. M., Cho, J., Madou, M., & Thong, K. L. (2018). A microdevice for rapid, monoplex and colorimetric detection of foodborne pathogens using a centrifugal microfluidic platform. *Biosensors and Bioelectronics, 100*, 96–104. https://doi.org/10.1016/j.bios.2017.08.060.

Sheng, W., Huang, N.a., Liu, Y., Zhang, B., Zhang, W., & Wang, S. (2020). An ultrasensitive fluorescence immunoassay based on magnetic separation and upconversion nanoparticles as labels for the detection of chloramphenicol in animal-derived foods. *Food Analytical Methods., 13*(11), 2039–2049. https://doi.org/10.1007/s12161-020-01820-5.

Wang, J., Wang, X., Tang, H., Gao, Z., He, S., Li, J., & Han, S. (2018). Ultrasensitive electrochemical detection of tumor cells based on multiple layer CdS quantum dots-functionalized polystyrene microspheres and graphene oxide - polyaniline composite. *Biosensors and Bioelectronics, 100*, 1–7. https://doi.org/10.1016/j.bios.2017.07.077.

Wang, S., Zheng, L., Cai, G., Liu, N., Liao, M., Li, Y., … Lin, J. (2019). A microfluidic biosensor for online and sensitive detection of *Salmonella typhimurium* using fluorescence labeling and smartphone video processing. *Biosensors and Bioelectronics, 140*, 111333. https://doi.org/10.1016/j.bios.2019.111333.

Wang, X., Yuan, W., Xu, Y., Yuan, H., & Li, F. (2020). Sensitive multiplex detection of MicroRNAs based on liquid suspension nano-chip. *Analytica Chimica Acta, 1112*, 24–33. https://doi.org/10.1016/j.aca.2020.03.026.

Xia, Y., Chen, Y., Tang, Y., Cheng, G., Yu, X.u., He, H., … Zheng, S.-Y. (2019). Smartphone-based point-of-care microfluidic platform fabricated with a ZnO nanorod template for colorimetric virus detection. *ACS Sensors, 4*(12), 3298–3307. https://doi.org/10.1021/acssensors.9b0192710.1021/acssensors.9b01927.s001.

Xing, K.-Y., Peng, J., Shan, S., Liu, D.-F., Huang, Y.-N., & Lai, W.-H. (2020). Green enzyme-linked immunosorbent assay based on the single-stranded binding protein-assisted aptamer for the detection of mycotoxin. *Analytical Chemistry, 92*(12), 8422–8426. https://doi.org/10.1021/acs.analchem.0c0107310.1021/acs.analchem.0c01073.s001.

Yin, J., Zou, Z., Hu, Z., Zhang, S., Zhang, F., Wang, B., … Mu, Y. (2020). A "sample-in-multiplex-digital-answer-out" chip for fast detection of pathogens. *Lab on a Chip, 20*(5), 979–986. https://doi.org/10.1039/C9LC01143A.

Zhao, X., Li, M., & Liu, Y. (2019). Microfluidic-based approaches for foodborne pathogen detection. *Microorganisms, 7*(10), 381. https://doi.org/10.3390/microorganisms7100381.

Zheng, L., Cai, G., Qi, W., Wang, S., Wang, M., & Lin, J. (2020). Optical biosensor for rapid detection of *Salmonella typhimurium* based on porous gold@platinum nanocatalysts and a 3D fluidic chip. *ACS Sensors, 5*(1), 65–72. https://doi.org/10.1021/acssensors.9b0147210.1021/acssensors.9b01472.s00110.1021/acssensors.9b01472.s002.

Zhang, C., Lv, X., Yasmeen, S., Qing, H., & Deng, Y. (2017). Integrated microfluidic chip with nanobiosensor for rapid and label-free detection of a specific gene. *Analytical Methods, 9*(24), 3619–3625. https://doi.org/10.1039/C7AY00950J.

Zheng, L., Cai, G., Wang, S., Liao, M., Li, Y., & Lin, J. (2019). A microfluidic colorimetric biosensor for rapid detection of *Escherichia coli O157:H7* using gold nanoparticle aggregation and smart phone imaging. *Biosensors and Bioelectronics, 124–125*, 143–149. https://doi.org/10.1016/j.bios.2018.10.006.